

Paper No.
16753



**Note on Selecting DC Potentials for EIS Measurements:
an Example of Determining the Diffusion Coefficient of Hydrogen Ion in Aqueous Solutions**

Negar Moradighadi, Bruce Brown and Srdjan Nestic

Institute for Corrosion and Multiphase Technology
Department of Chemical & Biomolecular Engineering, Ohio University
Athens, OH 45701

ABSTRACT

Electrochemical impedance spectroscopy (EIS) is a powerful technique that can detect and provide information about different phenomena that occur on the corroding surface using alternating current signals. Several electrochemical reactions and associated phenomena, such as mass transfer and chemical reactions happening at and near the metal surface, occur simultaneously. Therefore, the EIS data conducted at a specific DC potential often contain mixed information about several of those reactions, while at other potentials the EIS data are dominated by a single electrochemical reaction. To be able to focus on a single electrochemical reaction and its associated phenomena, it is important to identify the DC potential at which the EIS data provide the most relevant information about this reaction, otherwise, the analysis of the impedance data becomes very difficult. This work aims to show an example of how to select the DC potential range at which the hydrogen evolution reaction is dominant. Following this step, the EIS data can be used to determine the diffusion coefficient of hydrogen ion in a strong acid aqueous solution.

INTRODUCTION

EIS is a powerful tool, yet a challenging technique for studying of a corrosion electrochemical system. It can provide a broad range of information by decoupling the phenomena that occur at or near the metal surface¹⁻⁵. In the study of corrosion of mild steel in a strong acid solution, the main electrochemical reactions are anodic dissolution of iron and the cathodic reduction of hydrogen ions and water (at lower potentials). In EIS studies of these electrochemical reactions, choosing the appropriate DC potential is of great importance. For example, to study the hydrogen reduction reaction, which is often controlled by the mass transfer of hydrogen ions, a DC

potential must be chosen at which the EIS response provides mostly information about the hydrogen reduction reaction and the influence of other reactions on measured impedance is minimized. It is well known that at potentials below the open circuit potential (OCP), the measured current is dominated by hydrogen ion reduction. We are compelled to conclude that the impedance at these same potentials below the OCP is also dominated by the hydrogen reduction reaction? But, is this always the case?

In this work, a DC potential range in which the impedance associated with the hydrogen evolution reaction is dominant will be determined by building a model to determine the resistance of the key electrochemical reactions involved in the corrosion process: iron oxidation, hydrogen reduction and water reduction. Next, the EIS data, obtained at the determined DC potential, will be analyzed using a method explained in the literatures ^{1,6} to determine the diffusion coefficient of the hydrogen ion in a strong acid solution.

Theory Behind Calculation of Diffusion Coefficients

For an electrochemical reaction that depends both on potential and metal surface concentration of electroactive species, the faradic impedance is related to it is a faradic resistance in series with a diffusion impedance as shown in Figure 1 ¹.

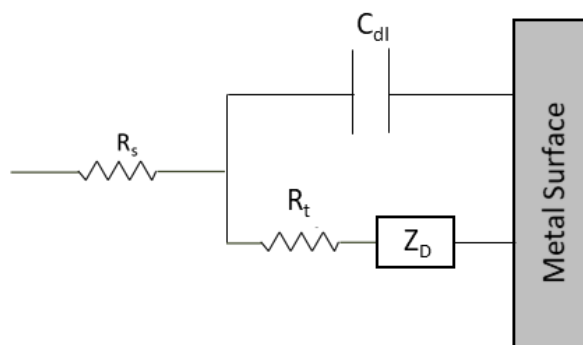


Figure 1. The schematic of the Randles circuit representing the surface phenomena and faradic reactions depending on potential and concentration of species at the metal surface.

As shown in Figure 1, the faradic impedance (Z_F) is a summation of faradic resistance (R_t) and diffusion impedance (Z_D) as shown in Equation (1) where Z_D is defined in Equation (2) ¹.

$$Z_F = R_t + Z_D \quad (1)$$

$$Z_D = R_D \left(-\frac{1}{\theta_i(0)} \right) \quad (2)$$

In Equation (2), R_D is a diffusion resistance, $\theta_i(0)$ is defined as a dimensionless concentration (Equations (3)) and $\theta'_i(0)$ is its first derivative with respect to distance from the surface (Equations (4))¹.

$$\theta_i(0) = \frac{\tilde{c}_i(y)}{\tilde{c}_i(0)} \quad (3)$$

$$\theta'_i(0) = \frac{d\left(\frac{\tilde{c}_i}{\tilde{c}_i(0)}\right)}{d\left(\frac{y}{\delta}\right)} \quad (4)$$

To analyze the derivative of concentration with respect to time and position, a convective-diffusion equation will be used as shown in Equation (5). Moreover, any complex value such as concentration can be defined by Equation (6) having a steady state and transient part. By substituting the first derivative of Equation (6) with respect to time and distance into Equation (5), and also considering the axial velocity profile near the surface of a rotating disk electrode (Equation (7)), the dimensionless form of the convective-diffusion equation can be obtained as shown in Equation (8). The dimensionless parameters in Equation (8) are defined in Equations (9)-(11)^{1,6}.

$$\frac{\partial c_i}{\partial t} + v_y \frac{\partial c_i}{\partial y} - D_i \frac{\partial^2 c_i}{\partial y^2} = 0 \quad (5)$$

$$c_i(y) = \bar{c}_i(y) + Re\{\tilde{c}_i e^{j\omega t}\} \quad (6)$$

$$v_y = -\sqrt{\nu\Omega} \left(\frac{-a\Omega}{\nu} y^2 + \frac{1}{3} \left(\frac{\Omega}{\nu} \right)^{3/2} y^3 + \frac{b}{6} \left(\frac{\Omega}{\nu} \right)^2 y^4 + \dots \right) \quad (7)$$

$$\frac{d^2 \theta_i}{d\xi^2} + \left(3\xi^2 - \left(\frac{3}{a^4} \right)^{1/3} \frac{\xi^3}{Sc_i^{1/3}} - \frac{b}{6} \left(\frac{3}{a} \right)^{5/3} \frac{\xi^4}{Sc_i^{2/3}} \right) \frac{\partial \theta_i}{\partial \xi} - jK_i \theta_i = 0 \quad (8)$$

$$\xi = \frac{y}{\delta_i} \quad (9)$$

$$K = 3.2576 p Sc^{1/3} \quad (10)$$

$$p = \frac{\omega}{\Omega} \quad (11)$$

Considering the boundary conditions shown below, Equation (8) can be solved by Newman, *et al.*⁷ method. Therefore the second term in the diffusion impedance (Z_D) was determined as shown in Equation (12)^{1,6}.

$$\theta_i \rightarrow 0 \text{ as } \xi \rightarrow \infty$$

$$\theta_i \rightarrow 1 \text{ at } \xi = 0$$

$$-\frac{1}{\theta_i(0)} = \Gamma\left(\frac{4}{3}\right) [1 + 0.298Sc^{-1/3} + 0.145Sc^{-2/3} + (pSc^{1/3})^2 \alpha + j(pSc^{1/3})\beta] \quad (12)$$

According to Tribollet *et al.*, the slope of the plot shown in Figure 2 is a function of the Schmidt number as shown in Equations (13) and (14). Once the Schmidt number is obtained the diffusion coefficient can be calculated using Equation (15)^{1,6}.

$$\lim_{p \rightarrow 0} \left(\frac{dRe \left\{ -\frac{1}{\theta_i(0)} \right\}}{dpIm \left\{ -\frac{1}{\theta_i(0)} \right\}} \right) = \lambda Sc^{1/3} \quad (13)$$

$$\lambda = 1.2261 + 0.84Sc^{-1/3} + 0.63Sc^{-2/3} \quad (14)$$

$$Sc = \frac{\nu}{D} \quad (15)$$

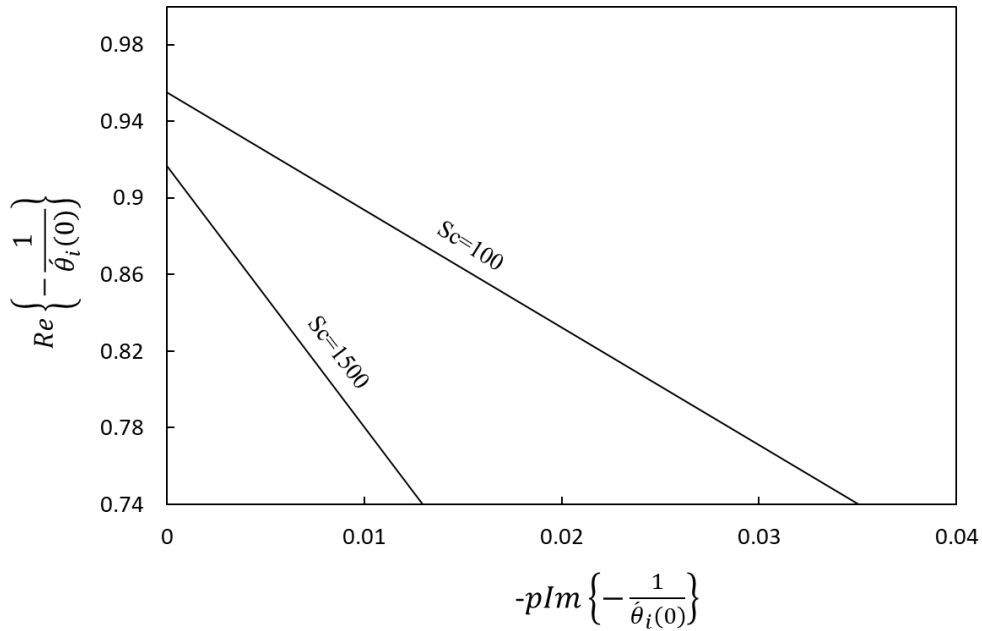


Figure 2. Determining the Schmidt number from the complex value of $\left(-\frac{1}{\theta_i(0)}\right)^{\beta}$.

METHODOLOGY

The first part of the experimental method is related to determining the DC potential at which the impedance is dominated by the hydrogen reduction reaction. The test conditions are shown in Table 1. A 3-electrode glass cell system with a rotating disk electrode is used for electrochemical experiments. The reference electrode is saturated KCl, Ag/AgCl. The counter and working electrodes are graphite and API 5L X65 mild steel respectively. Initially, the test solution is sparged with 1 bar N₂ for one hour to remove the oxygen content. The pH of the solution is adjusted using a dilute HCl solution. The metal sample is polished up to 1200 grit silicon carbide paper. Following polishing, the sample was mirror finished using a 0.25 diamond suspension liquid to avoid the generation of bubbles on the metal surface during the experiment. The sample was cleaned in an isopropanol liquid using ultrasonic for 2-3 minutes and then dried using N₂ stream.

Table 1. Experimental Conditions

Parameters	Values	
Test apparatus	Rotating disk electrode Three-electrode glass cell	
Sparged gas	pN ₂ ≈ 1 bar	
Temperature	30 ± 0.5 °C	
pH	3.00 ± 0.01	
Supporting electrolyte	0.1 M NaCl	
Rotation rate	1000, 2000, 3000 rpm	
Electrode material	API 5L X65	
Parameters of the EIS scans		
Frequency	10000 to 0.001 Hz	
AC potential	10 mV rms.	
DC potential	Rotation speed	DC potential
	1000 rpm	-250 mV vs. OCP
	2000 rpm	-290 mV vs. OCP
	3000 rpm	-290 mV vs. OCP

After the insertion of the sample in the glass cell, the open circuit potential (OCP) was monitored for 20 minutes to obtain a constant value (DOCP < +/- 0.1 mV/min), and then cathodic potentiodynamic polarization measurement was performed. In the next step, the sample was taken out of the glass cell to polish and mirror finish it again. Then after the insertion of the sample in the solution, OCP was monitored for 20 minutes and then anodic potentiodynamic polarization was performed.

The analysis method of the potentiodynamic sweeps for determination of DC potential for EIS measurement is described in the result and discussion and the values are shown in Table 1. EIS experiments were performed in a fresh solution following the solution and sample preparation procedure described above and in Table 1. After insertion of the sample in the solution and obtaining a constant value of OCP, the EIS experiments were performed at -250 mV vs. OCP at 1000 rotation speed of working electrode and at -290 mV vs. OCP at 2000 and 3000 rotation speeds.

RESULT AND DISCUSSION

Determining of the DC potential for EIS measurement

The measured potentiodynamic sweeps at three different rotation speeds are shown in Figure 3. In the next step, the measured sweeps were fitted to a mechanistically modeled

potentiodynamic sweep. An example of a measured sweep fitted to the model potentiodynamic sweep, deconvoluted to show the underlying electrochemical reactions, is shown in Figure 4.

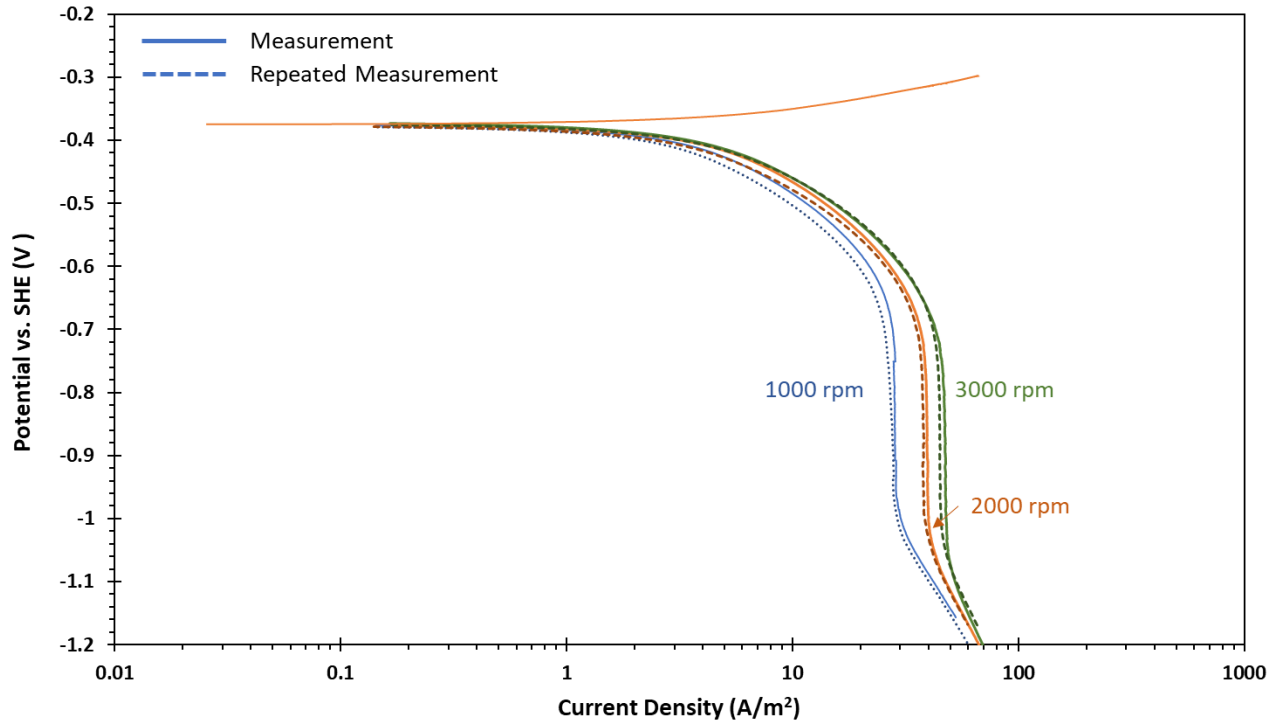


Figure 3. Steady-state polarization sweep curves, 30°C, pH 3.0, 0.1 M NaCl, sparged with nitrogen. The dotted line represents the repeated experiment.

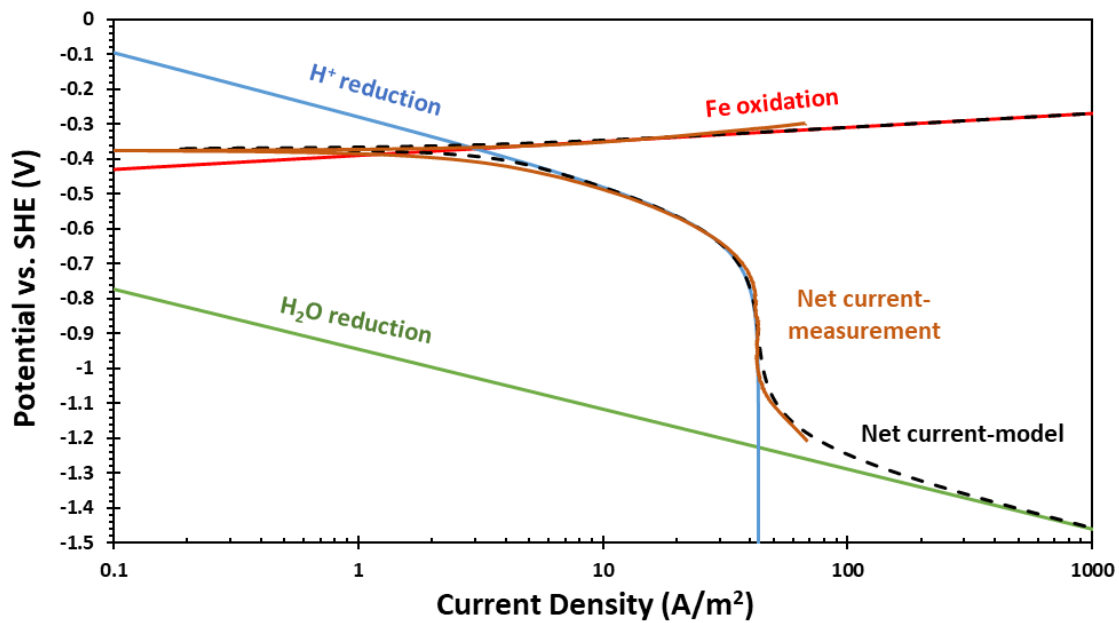


Figure 4. The fit of the experimental data to the modeled potentiodynamic data.

The model data was then used to estimate the polarization resistances of each of the electrochemical reaction for the process at various potentials. For each reaction (cathodic and

anodic), the resistance was calculated using Equation (16) at different potentials. Using the parallel resistor assumption for the electrochemical reactions, the overall resistance is calculated using Equation (17) which shows that the overall resistance is dominated by the smallest of the three resistances.

$$R = \frac{\Delta V}{\Delta I} \quad (16)$$

$$\frac{1}{R_{overall}} = \frac{1}{R_{Fe}} + \frac{1}{R_{H^+}} + \frac{1}{R_{H_2O}} \quad (17)$$

By inspection of the data presented in Figure 5, the range of potentials where the net resistance is dominated by the H⁺ reduction reaction resistance, is in the range between -60 mV and -450 mV vs OCP as shown by the blue box. In other words, in this range of potentials, the contribution of the impedance of the iron oxidation and water reduction to the overall impedance is very small and therefore the measured impedance can be considered as the response of the hydrogen reduction reaction, as shown in Figure 7.

The same range of potentials is shown on the plot of potentiodynamic data presented in Figure 6. This analysis shows that not the whole cathodic potential range (more negative than the OCP) is suitable for EIS measurement in order to determine the impedance related to the hydrogen ion reduction reaction. At the potential range from OCP to -60 mV below the OCP the current is dominated by the H⁺ reduction being under charge transfer control; however, the impedance is dominated by the anodic reaction having the smallest resistance value of the resistance of all three electrochemical reactions. Moreover, at potential -450 mV below OCP, the impedance is dominated by the water reduction although the current is still dominated by the H⁺ reduction and being controlled by mass transfer of H⁺ ion.

The same analysis was performed for the experimental data at rotation speeds of 1000 and 3000 rpm. For the EIS measurement, the potential of -250 mV vs. OCP was chosen for 1000 rpm and -290 mV vs. OCP was chosen for 2000 and 3000 rpm.

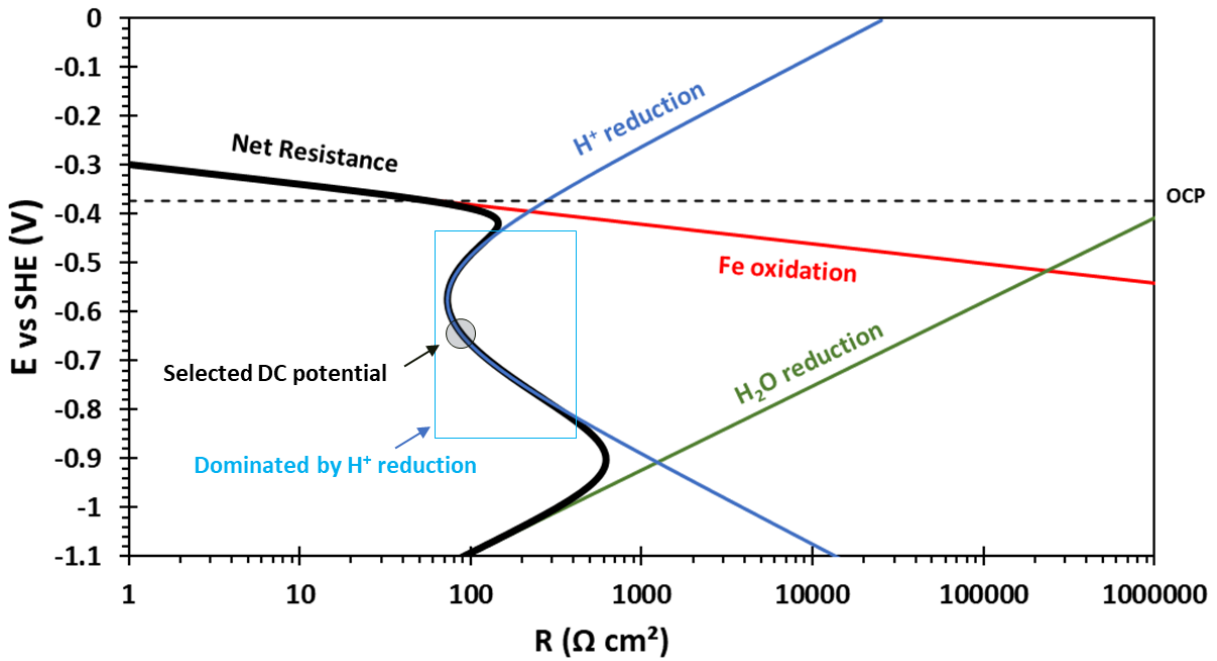


Figure 5. The calculated polarization resistance as a function of potential for experimental data at 1 bar N_2 , pH 3, $T = 30^\circ C$, 0.1 M NaCl, and 2000 rpm.

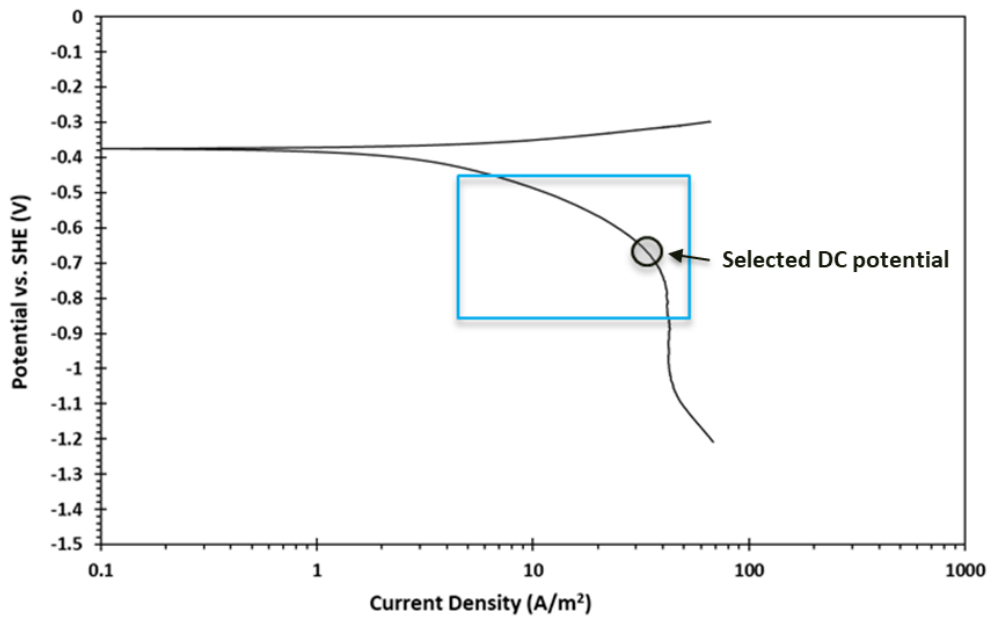


Figure 6. Potentiodynamic sweep for the experiments at 1 bar N_2 , pH 3, $T = 30^\circ C$, 0.1 M NaCl, and 2000 rpm. The blue box represents the potential range at which the impedance of the cathodic reaction, H^+ reduction, is dominant for EIS measurements.

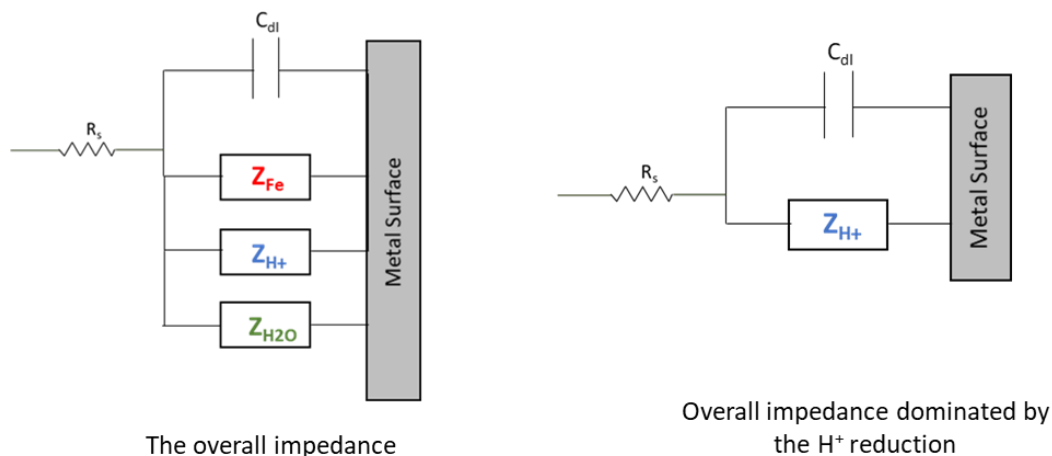


Figure 7. The schematic of the Randles circuit. The figure on the left side is the overall impedance. The figure on the right side is the overall impedance at the potential range dominated by the H⁺ reduction

Determining the Schmidt Number from the Data in the Low Frequency Range

Figure 8 shows the impedance data for experimental data at rotation speeds of 1000, 2000, and 3000 rpm. Each Nyquist plot represents two-time constants. The high-frequency loop (near the origin) corresponds to a capacitive loop while the low-frequency loop is related to the diffusion impedance. The data shown in Figure 8, were normalized with respect to the corrected real part of the impedance data according to Tribollet *et al.* Method ^{1,6}, as shown in Figure 9.

According to Tribollet *et al.* the p value was calculated using Equation (18) ^{1,6}. Based on the analysis discussed, the slope of the low frequency data shown in Figure 10 yields information about the Schmidt number using Equations (13) and (14). The linear portion of the plot on the left hand side of Figure 10 yields a slope of -6.2 ± 0.4 , which corresponds to a Schmidt number of 97 ± 19 . Finally, by using Equation (15), the diffusion coefficient of hydrogen ions in water is calculated to be $8.6 \times 10^{-5} \pm 1.6 \times 10^{-5} \text{ cm}^2/\text{s}$.

$$p = \frac{\omega}{\Omega} = \frac{60 \times f}{(rpm)} \quad (18)$$

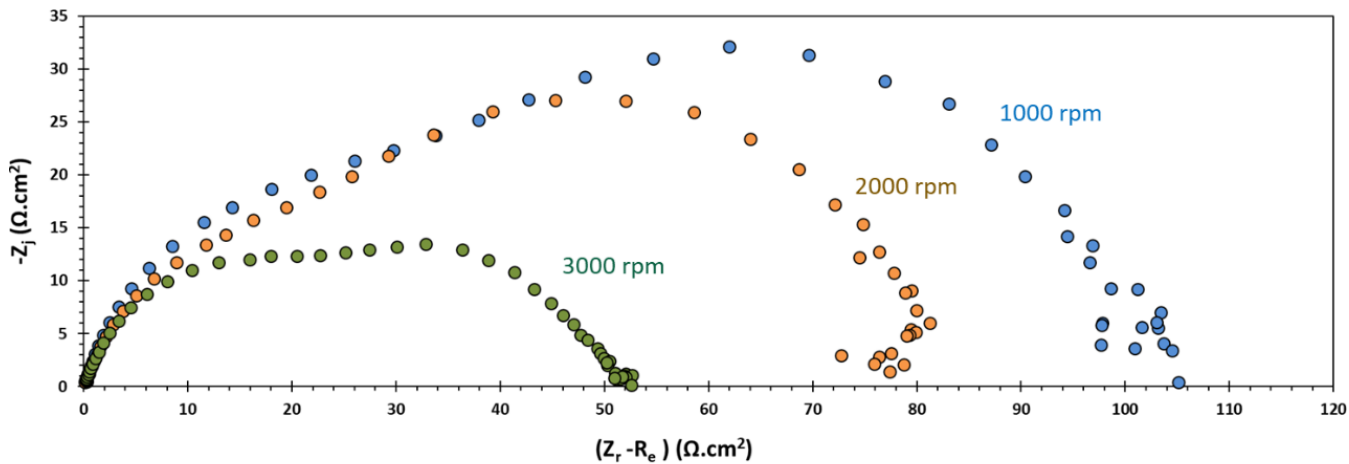


Figure 8. Impedance data at different rotation speeds from the experiments at 1 bar N₂, pH 3, T= 30°C, 0.1 M NaCl.

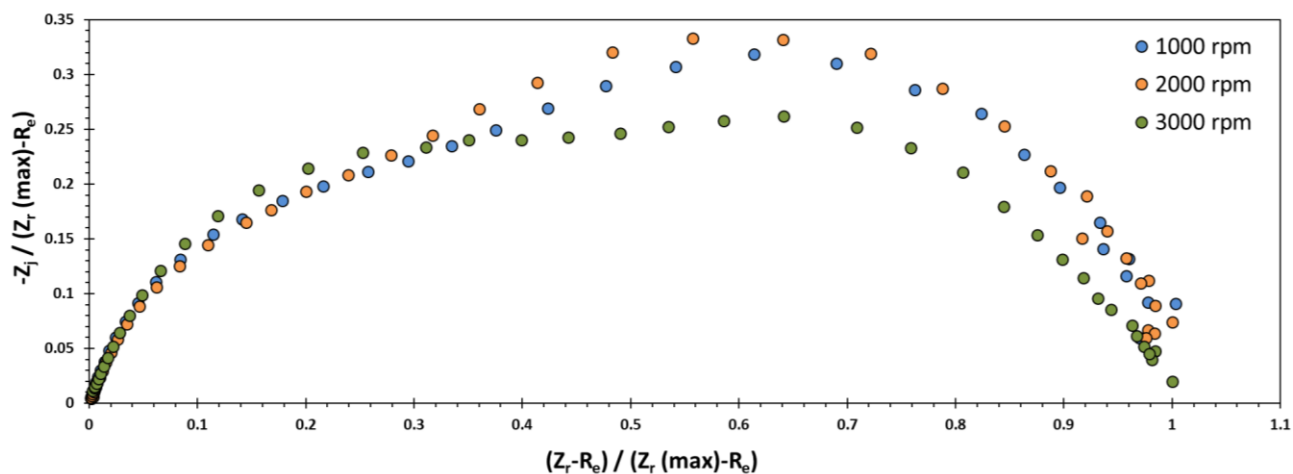


Figure 9. Normalized impedance data from Figure 8.

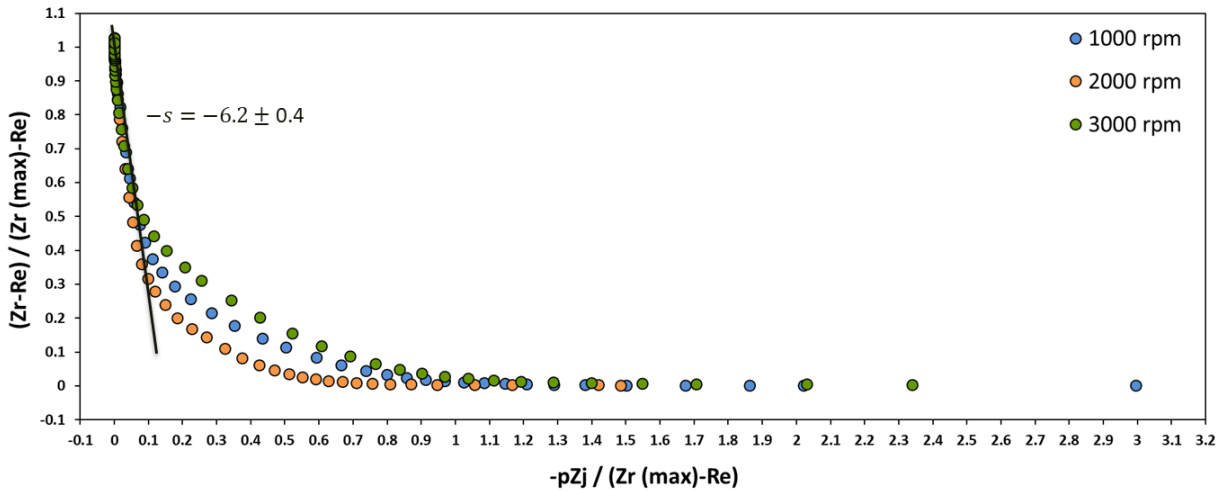


Figure 10. Illustration of the method developed by Tribollet et al. to determine the Schmidt number S from the normalized data in Figure 9.

Determining the diffusion coefficient using potentiodynamic sweeps (DC technique)

The diffusion coefficient of the hydrogen ion in water was initially determined using potentiodynamic sweeps in order to compare with the value obtained by the EIS technique. The pure mass transfer controlled limiting current on a rotating disk electrode can be calculated using the Levich equation shown as Equation (19) ⁸. Therefore, the rate of change in limiting current with respect to square root of rotation speed carries information about the diffusion coefficient of the electroactive species, being H^+ ion in this study.

$$i_{lim} = 0.62nFD^{2/3}v^{-1/6} C_b \omega^{1/2} \quad (19)$$

The value of limiting current obtained in the potentiodynamic experiments shown in Figure 3 is plotted versus the square root of the rotation speed, which, according to Equation (19), it appears that it needs to pass through the origin; meaning that at zero rotation speed (stagnant condition), the limiting current must be equal to zero. Actually, at a stagnant condition there is still mass transfer due to molecular diffusion of the hydrogen ion and therefore, the limiting current must be a small with value close to zero. Based on Equation (19), the slope of the line shown in Figure 3, $\tan(\alpha)$, is equivalent to the term $0.62nFD^{2/3}v^{-1/6} C_b$. Solving for the diffusion coefficient, D , provides Equation (20). According to Equation (20), the diffusion coefficient of hydrogen ion in water is $9.3 \times 10^{-5} \pm 0.3 \times 10^{-7} \text{ cm}^2/\text{s}$.

$$D = \left[\frac{\tan(\alpha) v^{1/6}}{0.62nFC_b} \right]^{3/2} \quad (20)$$

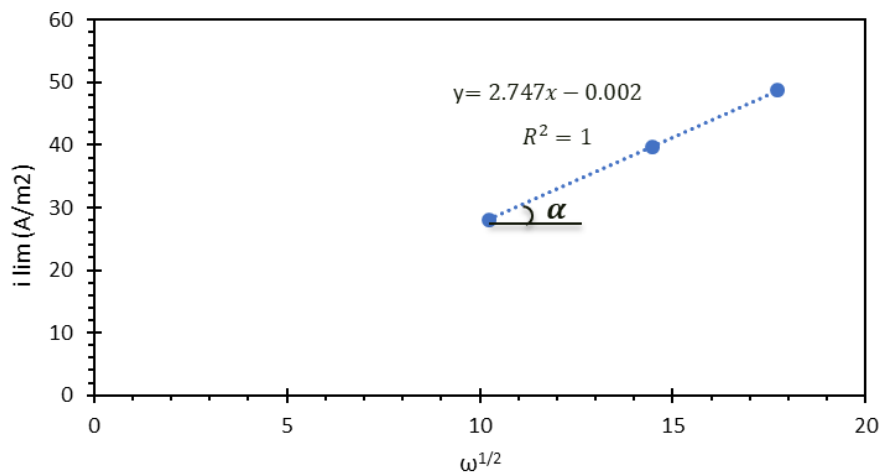


Figure 11. Using the limiting current density values, shown in Figure 3, to determine the diffusion coefficient of hydrogen ion using Equation (19).

Comparison of the Diffusion Coefficients Obtained by EIS and Potentiodynamic Sweeps

The diffusion coefficient for the hydrogen ion in water obtained by EIS and potentiodynamic sweeps are $8.6 \times 10^{-5} \pm 1.6 \times 10^{-5}$ and $9.3 \times 10^{-5} \pm 0.3 \times 10^{-7}$ respectively. The calculated error and difference between the two values is $18 \pm 8 \%$. The error might correspond to the impact of impedance related to other electrochemical reactions happening simultaneously on the metal surface. As discussed, at the chosen potential, the measured impedances are dominated by the H^+ ion reduction; however, there are still small contributions from the iron dissolution reaction and water reduction reaction to the measured impedance which might be responsible for the calculated error. The two values obtained for diffusion coefficient of hydrogen ion in water can also be compared to 12×10^{-5} (cm^2/s), which is the value reported in literature^{9,10}. The difference and error between the measured values and the one reported in the literature are shown in Table 2.

Table 2. Comparison of the Measured Diffusion Coefficients with the Literature Value

Measurement technique	Measured D_{H^+} (cm^2/s)	Error between the measured D_{H^+} and the value reported in the literature: 12×10^{-5} (cm^2/s) ^{9,10}
EIS	$8.6 \times 10^{-5} \pm 1.6 \times 10^{-5}$	$29 \pm 14 \%$
Potentiodynamic sweep	$9.3 \times 10^{-5} \pm 0.3 \times 10^{-7}$	22.5 %

CONCLUSIONS

- DC potential range at which the impedance of hydrogen evolution reaction is dominant was determined using potentiodynamic polarization sweeps data. At the selected DC potential, the EIS experiments were performed to determine the diffusion coefficient of the hydrogen ions.
- The diffusion coefficient values obtained from the EIS method were close to the value obtained by the DC technique with 18 ± 8 % of error and similar to the reported literature value with 29 ± 14 % of error.

ACKNOWLEDGEMENTS

We would like to thank Dr. Bernard Tribollet for his guidance and comments in analysis of the experimental results. Moreover, the author would like to acknowledge the following companies for their financial support: Baker Hughes, BP, Chevron, Clariant Corporation, CNOOC, ConocoPhillips, ExxonMobil, M-I SWACO (Schlumberger), Multi-Chem (Halliburton), Occidental Oil Company, Pioneer Natural Resources, Saudi Aramco, Shell Global Solutions, SINOPEC (China Petroleum), and TOTAL.

REFERENCES

1. Orazem, M.E., and B. Tribollet, *Electrochemical Impedance Spectroscopy*, 2nd ed. (Hoboken, NJ: John Wiley & Sons, Inc., 2017).
2. das Chagas Almeida, T., M.C.E. Bandeira, R.M. Moreira, and O.R. Mattos, *Corrosion Science* 120 (2017): pp. 239–250.
3. Keddam, M., O.R. Mattos, and H. Takenouti, *J. Electrochem. Soc.* 128 (1981): p. 257.
4. Keddam, M., O.R. Mattos, and H. Takenouti, *J. Electrochem. Soc.* 128 (1981): p. 266.
5. Hirschorn, B., M.E. Orazem, B. Tribollet, V. Vivier, I. Frateur, and M. Musiani, *Electrochimica Acta* 55 (2010): pp. 6218–6227.
6. Tribollet, B., J. Newman, and W.H. Smyrl, *J. Electrochem. Soc.* 135 (1988): pp. 134–138.
7. Newman, J., and K.E. Thomas-Alyea, *Electrochemical Systems* (John Wiley & Sons, 2012).
8. Levich, V.G., *Physicochemical Hydrodynamics* (Englewood Cliffs, N.J: Prentice-Hall, 1969).
9. Kahyarian, A., M. Achour, and S. Nestic, “34 - Mathematical Modeling of Uniform CO₂ Corrosion,” in *Trends in Oil and Gas Corrosion Research and Technologies*, ed. A.M. El-Sherik (Boston: Woodhead Publishing, 2017), pp. 805–849.
10. Atkins, P.W., *Physical Chemistry*, 2nd ed. (Oxford, England: Oxford University Press, 1982).